Received ; | Revised ; | Accepted

DOI: xxx/xxxx

RESEARCH ARTICLE

Riemann problem for constant flow with single-point heating source[†]

Changsheng Yu | Chengliang Feng | Zhiqiang Zeng | Tiegang Liu

[1]School of Mathematics, Beihang University, Beijing 100191, PR China

Correspondence
*Tiegang Liu, School of Mathematics, Beihang University, Beijing 100191, PR China. Email: liutg@buaa.edu.cn

This work focuses on the Riemann problem of Euler equations with global constant initial conditions and a single-point heating source, which comes from the physical problem of heating one-dimensional inviscid compressible constant flow. In order to deal with the source of Dirac delta-function, we propose an analytical frame of double classic Riemann problems(CRPs) coupling, which treats the fluids on both sides of the heating point as two separate Riemann problems and then couples them. Three structures of the exact Riemann solution are found, which is consistent with the results of numerical methods. Furthermore, we establish the uniqueness of the Riemann solution with some restrictions on the Mach number of the initial condition.

KEYWORDS:
hyperbolic balance law, δ-singularity, Riemann problem

1 | INTRODUCTION

The Riemann problem of the one-dimensional inviscid compressible flow with global constant initial conditions and a singe-point heating source is studied in this paper. The heating point is located at $x = 0$. The governing equations is given by

$$\frac{\partial U}{\partial t} + \frac{\partial F}{\partial x} = S, \tag{1}$$

where

$$U = \begin{pmatrix} \rho \\ \rho u \\ E \end{pmatrix}, F = \begin{pmatrix} \rho u \\ \rho u^2 + p \\ (E + p)u \end{pmatrix}, S = \begin{pmatrix} 0 \\ 0 \\ Q\delta(x) \end{pmatrix}.$$

Here, ρ, p and E denote the thermodynamical variables: density, pressure and total energy, respectively. u is velocity. $Q > 0$ is the heat flux per unit time added to the flow. $\delta(x)$ is the Dirac delta-function. Therefore, the source means that Q heat is added to the flow from the heating point per unit time. We assume that the fluid is polytropic ideal and the equaiotn of state is given by

$$p = (\gamma - 1)\rho e, \quad 1 \le \gamma \le 3.$$

where γ is the ratio of specific heats and e is the internal energy. The initial condition is

$$U(x, 0) \equiv U_1 = (\rho_1, \rho_1 u_1, E_1), \tag{2}$$

where ρ_1, u_1 and E_1 are constant. We assume that u_1 is greater than 0 for convenience. The subscript 1 represents the initial condition in this paper. The physical problem described by the Riemann problem (1.1)-(1.2) is that Q heat is added to the one-dimensional constant flow per unit time, as shown in Figure 1.

[†]This work is supported by the NSFC -NSAF joint fund, No. U1730118 and Science Challenge Project, No. JCKY2016212A502.

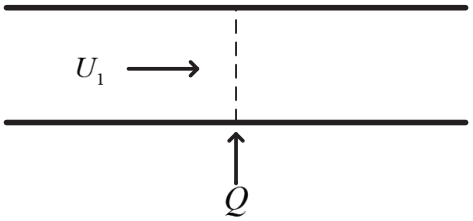

FIGURE 1 one-dimensional constant flow with heat addition from a single point

We use the subscripts $-$ and $+$ to represent the limiting states upstream and downstream of the heating point respectively. We set

$$U_-(t) = U(0-,t), \quad U_+(t) = U(0+,t).$$

The source term implies a jump of the energy flux across the heating point:

$$\begin{aligned} \rho_-(t)u_-(t) &= \rho_+(t)u_+(t) \\ \rho_-(t)u_-(t)^2 + p_-(t) &= \rho_+(t)u_+(t)^2 + p_+(t) \\ (E_-(t) + p_-(t))u_-(t) + Q &= (E_+(t) + p_+(t))u_+(t). \end{aligned} \tag{3}$$

If the velocity at the heating point is zero, thermal convection does not occur, and the added heat has no effect on the surrounding flow. Thus in the following paper we assume that

$$u_-(t) \neq 0, \quad u_+(t) \neq 0.$$

We will prove that the solution of Riemann problem (1.1)-(1.2) is self-similar in the third section, therefore both $U_-(t)$ and $U_+(t)$ are constant vectors. Omitting the time parameter t, we can get the following equation from (1.3):

$$\left(\frac{1}{2}{u_-}^2 + h_-\right)(1+k) = \frac{1}{2}{u_+}^2 + h_+,$$

where h is enthalpy, $k = \frac{Q}{\rho_-(t)u_-(t)\left(\frac{1}{2}{u_-}^2+h_-\right)}$ is assumed to be a constant parameter.

We call following equations the heating equations:

$$\begin{cases} \rho_- u_- = \rho_+ u_+ \\ \rho_- {u_-}^2 + p_- = \rho_+ {u_+}^2 + p_+ \\ \left(\frac{1}{2}{u_-}^2 + h_-\right)(1+k) = \frac{1}{2}{u_+}^2 + h_+ \end{cases}. \tag{4}$$

The solution of the heating equations (1.4) corresponds to the steady solution of Riemann problem (1.1)-(1.2). Therefore, the properties of the solution of the heating equations (1.4) are important for the study of Riemann problem (1.1)-(1.2).

The mathematical model of Figure 1 can be applied to the study of one-dimensional condensation problem [1,2]. The condensation of the vapor leads to the release of latent heat and therefore has heating effects on the carrier fluid. Previous researches on condensation problems have revealed some information about the solution of Riemann problem (1.1)-(1.2). The solution of the heating equations (1.4), which is a steady solution of the Riemann problem, has already been available [1,3,2,4]. In [4] Schnerr made a good summary of the properties of the solution of (1.4) with $M_- > 1$, which is typical for condensation problems. Schnerr showed that there are two solutions of the heating equations (1.4), one called the shock solution, which reduces to identity with $Q = 0$, and the other called the weak solution, which reduces to the adiabatic normal shock solution with $Q = 0$. For the heat addition of subsonic flow, Schnerr predicted the appearance of the unsteady solution, but did not do a more detailed analysis. There are other solution expressions of the heating equations. For example, Delale [1,3] and Dongen [2] have their own forms of the solution of (1.4). For the unsteady solution of the Riemann problem, some scholars have proposed the possible wave patterns of the solution, but the complete and rigorous theoretical proof is lacking at present. Dongen [2] studied the unsteady effects of

the heat addition, and proposed three possible solution structures. Those three structures are determined by the Mach numbers of the fluid around the heating point. Numerical simulation is an effective method to explore the wave patterns of the heating problem. Chengwan[5] used the ASCE method[6] to numerically verify the above three structures by the simulation of the onset of condensation in a slender Laval nozzle. In the wet nitrogen condensation problem of the Laval nozzle, Chengwan showed the transition between the three structures by adjusting the humidity. However, the above work focused on using numerical methods to reveal some of the properties of the heating problem. To our knowledge, there is no effective theoretical method to study the exact solution of Riemann problem (1.1)-(1.2).

Riemann problem (1.1)-(1.2) has two features: first, the initial condition is global constant; second, the governing equations are non-homogeneous equations containing a δ-singularity source term. The second property is the key point, which has an essential impact on the structure of the solution. One way to deal with Riemann problems with source terms is called generalized Riemann problem(GRP)[7,8] or derivative Riemann problem(DRP)[9,10]. The Riemann problem of homogeneous Euler equations with piecewise constant initial conditions is also called classical Riemann problem(CRP). Based on the exact solution of CRP, GRP made two extensions: the initial condition is changed from piecewise constant functions to piecewise linear functions or even piecewise smooth functions; the governing equations become non-homogeneous equations containing source terms. GRP can solve many Riemann problems with complex source terms, such as the Riemann problem of shallow water equations[11] and the Riemann problem of three-dimensional spherically symmetric equations[12]. However, the sources are assumed to be smooth functions by default in those GRP solvers. As a result, the source term affects the Riemann solution in the second and higher space-time order. That is, the effect of sources will disappear when the time tends to zero. Therefore the wave patterns of the GRP solution are the same as the wave patterns of its corresponding CRP solution. For Riemann problem (1.1)-(1.2), the existing GRP solvers can not be directly applied. The reason is that the source S is not a continuous function, which makes a huge effect on the Riemann solution at the beginning and directly changes the wave pattern. In fact, as can be seen from[1], the solution of Riemann problem (1.1)-(1.2) may be a three waves structure or a four waves structure, which is different from the zero wave structure of its CRP.

If the Dirac delta-function in the source term takes the form of the derivative of a step function, we have

$$\delta(x) = \frac{\partial h}{\partial x}.$$

An alternative definition of h is

$$h(x) = \begin{cases} 0, & x < 0 \\ 1, & x \geq 0 \end{cases}.$$

We can remove the obstacle of the source term by supplementing the system (1.1) with the trivial equation:

$$\frac{\partial h}{\partial t} = 0. \tag{5}$$

The original Euler equations with source terms becomes the following hyperbolic equations without source terms:

$$\begin{cases} \dfrac{\partial \rho}{\partial t} + \dfrac{\partial (\rho u)}{\partial x} = 0 \\ \dfrac{\partial (\rho u)}{\partial t} + \dfrac{\partial (\rho u^2 + p)}{\partial x} = 0 \\ \dfrac{\partial E}{\partial t} + \dfrac{\partial (Eu + pu)}{\partial x} - Q\dfrac{\partial h}{\partial x} = 0 \\ \dfrac{\partial h}{\partial t} = 0 \end{cases}. \tag{6}$$

The new equation (1.5) gives rise to a new linearly degenerate characteristic field and a new stationary discontinuity. That seems to be an effective way to solve the Riemann problem (1.1)-(1.2). In fact, that method has been used by many scholars to deal with hyperbolic banlance problems with the source term of Dirac delta-function, such as the Riemann problem for the fluid in a nozzle with discontinuous cross-sectional area[13,14,15] and the Riemann problem for the shallow water equations with discontinuous topography[16,17,18,19]. Although that method can eliminate the source terms, the augmented system (1.6) is obviously not strictly hyperbolic. In addtion, if Q is related to the state of the fluid rather than a constant, then the augmented system (1.6) is non-conservative, just like the augmented hyperbolic system in[15]. Although the augmented equations do not contain source terms, the solution process of the Riemann problem is very complex and often be problem-related due to the

lack of conservation or strict hyperbolicity.

In this work, we propose an analytical frame of double CRPs coupling at the heating point to construct the exact solution of the Riemann problem (1.1)-(1.2). It regards the fluids on both sides of the heating point as two separate CRPs, and gives the upper limit of the number of waves first. The solutions of the two CRPs are then coupled on the premise of maintaining the physical properties of the heating point. Depending on the heating properties and gasdynamics properties, the extra waves are deleted and the type of wave is finally determined. One advantage of the double CRPs coupling method is that it is independent of whether the fluid at the heating point is supersonic or subsonic. Using the present method we demonstrate three possible structures of the solution, which are verified by examples in the sixth section.

The text is arranged as follows. In the second section, we will introduce the solution of the heating equations and derive several useful properties. In the third section, an analytical frame of double CRPs coupling will be introduced by solving the Riemann problem (1.1)-(1.2). We will use this method to prove the three structures of the exact solution. In teh forth section, we will give an iterative method for the exact solution of each structure. In the fifth section, the structure of the solution will be associated with the Mach number of the incoming flow to illustrate the uniqueness of the solution. In the sixth section, we will give five examples of the Riemann problem (1.1)-(1.2) with different initial conditions and heating coefficients to verify our results. Finally, a brief summary will be given in the seventh section.

2 | HEATING EQUATIONS

There are two different branches of the solution of the heating equations (1.4), but only one of them is physical. The physical solution satisfy the following criterion[20]:

Property 2.1. If $M_- < 1$, then $M_+ \le 1$. If $M_- > 1$, then $M_+ \ge 1$.

The physical solution corresponds to the weak solution in[4]. In this paper the solution of Dongen[2] is adopted. For the heat addition of subsonic flow, the solution is

$$I \equiv \sqrt{\left(\gamma + \frac{1}{{M_-}^2}\right)^2 - 2(\gamma+1)\left(\frac{1}{{M_-}^2} + \frac{\gamma-1}{2}\right)(1+\kappa)}, \tag{7a}$$

$$\frac{u_+}{u_-} = \frac{\rho_-}{\rho_+} = \frac{1}{\gamma+1}\left(\gamma + \frac{1}{{M_-}^2} - I\right), \tag{7b}$$

$$\frac{p_+}{p_-} = \frac{{M_-}^2}{\gamma+1}\left(\gamma + \frac{1}{{M_-}^2} + \gamma I\right), \tag{7c}$$

$$M_+ = \sqrt{\frac{\gamma + \frac{1}{{M_-}^2} - I}{\gamma + \frac{1}{{M_-}^2} + \gamma I}}. \tag{7d}$$

For the heat addition of supersonic flow, the solution is

$$I \equiv \sqrt{\left(\gamma + \frac{1}{{M_-}^2}\right)^2 - 2(\gamma+1)\left(\frac{1}{{M_-}^2} + \frac{\gamma-1}{2}\right)(1+\kappa)}, \tag{8a}$$

$$\frac{u_+}{u_-} = \frac{\rho_-}{\rho_+} = \frac{1}{\gamma+1}\left(\gamma + \frac{1}{{M_-}^2} + I\right), \tag{8b}$$

$$\frac{p_+}{p_-} = \frac{{M_-}^2}{\gamma+1}\left(\gamma + \frac{1}{{M_-}^2} - \gamma I\right), \tag{8c}$$

$$M_+ = \sqrt{\frac{\gamma + \frac{1}{{M_-}^2} + I}{\gamma + \frac{1}{{M_-}^2} - \gamma I}}. \tag{8d}$$

M is Mach number. The advantage is that the ratios of variables before and after heat addition are only related to the upstream Mach number of the heating point. In order to make the solution reasonable, there is an upper bound on k:

$$k \le k_{max} \overset{def}{=} \frac{(1-{M_-}^2)^2}{2(\gamma+1){M_-}^2\left(1 + \frac{\gamma-1}{2}{M_-}^2\right)}. \tag{9}$$

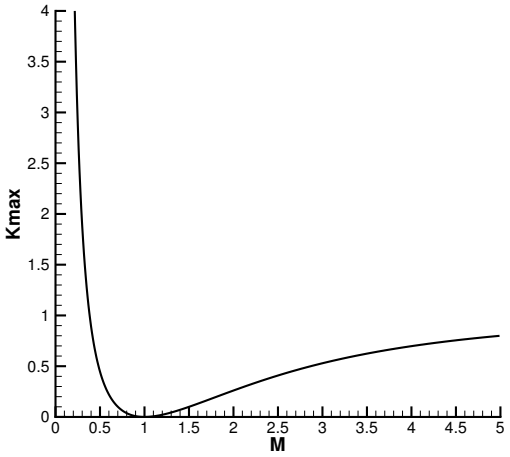

FIGURE 2 Relation between the maximum heat parameter and the Mach number of the flow upstream to the heating point.

k_{max} is called maximum heat parameter. The relation between k_{max} and M_- is shown in figure 2. For $M_- \to 0+$, k_{max} approaches asymptotically ∞. For $M_- \to \infty$, k_{max} approaches asymptotically a finite number $\frac{1}{\gamma^2-1}$. When k is a fixed number and $k < \frac{1}{\gamma^2-1}$, there are two numbers of M satisfy:

$$k = \frac{(1-M^2)^2}{2(\gamma+1)M^2\left(1 + \frac{\gamma-1}{2}M^2\right)}.$$

One of these two numbers is greater than 1, labeled M_{**}, and one is less than 1, labeled M_*. When $k \ge \frac{1}{\gamma^2-1}$, the solution of above equation is unique, which is labeled M_* and is less than 1. From the relation between M_- and k_{max}, we can draw the following conclusion:

Lemma 2.1. For a given k, we have:

(1) when $k < \frac{1}{\gamma^2-1}$, $M_- \le M_*$ or $M_- \ge M_{**}$;

(2) when $k \ge \frac{1}{\gamma^2-1}$, $M_- \le M_*$;

(3) If $M_- = M_*$ or $M_- = M_{**}$, $I = 0$ and $M_+ = 1$ hold.

The case of $M_+ = 1$ is called thermal choking state. At this time, the fluid becomes a sonic flow after being heated. As can be seen from Figure 2, any heat addition is not allowed for the sonic flow.

Theorem 2.1. $\frac{u_+}{u_-} > 1$, $\frac{p_+}{p_-} < 1$, $\frac{\rho_+}{\rho_-} < 1$ and $\frac{M_+}{M_-} > 1$ hold for the heat additon of subsonic flow. $\frac{u_+}{u_-} < 1$, $\frac{p_+}{p_-} > 1$,$\frac{\rho_+}{\rho_-} > 1$ and $\frac{M_+}{M_-} < 1$ hold for the heat addition of supsonic flow.

Proof. For the heat addition of subsonic fluid, $k > 0$ implies

$$I < \sqrt{\left(\gamma + \frac{1}{{M_-}^2}\right)^2 - 2(\gamma+1)\left(\frac{1}{{M_-}^2} + \frac{\gamma-1}{2}\right)} = \frac{1}{{M_-}^2} - 1,$$

$$\frac{u_+}{u_-} > \frac{1}{\gamma+1}\left(\gamma + \frac{1}{{M_-}^2} + 1 - \frac{1}{{M_-}^2}\right) = 1,$$

$$\frac{\rho_+}{\rho_-} = \frac{u_-}{u_+} < 1,$$

$$\frac{p_+}{p_-} < \frac{{M_-}^2}{\gamma+1}\left(\gamma + \frac{1}{{M_-}^2} - \gamma + \frac{\gamma}{{M_-}^2}\right) = 1,$$

$$M_+ = \sqrt{\frac{\gamma + \frac{1}{{M_-}^2} - I}{\gamma + \frac{1}{{M_-}^2} + \gamma I}} > \sqrt{\frac{\gamma + \frac{1}{{M_-}^2} - \frac{1}{{M_-}^2} + 1}{\gamma + \frac{1}{{M_-}^2} + \gamma(\frac{1}{{M_-}^2} - 1)}} = M_-.$$

For the heat addition of supsonic fluid, $k > 0$ implies

$$I < \sqrt{\left(\gamma + \frac{1}{{M_-}^2}\right)^2 - 2(\gamma+1)\left(\frac{1}{{M_-}^2} + \frac{\gamma-1}{2}\right)} = 1 - \frac{1}{{M_-}^2},$$

$$\frac{u_+}{u_-} < \frac{1}{\gamma+1}\left(\gamma + \frac{1}{{M_-}^2} + 1 - \frac{1}{{M_-}^2}\right) = 1,$$

$$\frac{\rho_+}{\rho_-} = \frac{u_-}{u_+} > 1,$$

$$\frac{p_+}{p_-} > \frac{{M_-}^2}{\gamma+1}\left(\gamma + \frac{1}{{M_-}^2} - \gamma + \frac{\gamma}{{M_-}^2}\right) = 1,$$

$$M_+ = \sqrt{\frac{\gamma + \frac{1}{{M_-}^2} + I}{\gamma + \frac{1}{{M_-}^2} - \gamma I}} < \sqrt{\frac{\gamma + \frac{1}{{M_-}^2} - \frac{1}{{M_-}^2} + 1}{\gamma + \frac{1}{{M_-}^2} + \gamma(\frac{1}{{M_-}^2} - 1)}} = M_-.$$

□

According to (2.1) and (2.2), $\frac{u_+}{u_-}$ and $\frac{p_+}{p_-}$ are both functions of M_-. For the subsonic heat addition, we set

$$\phi(M_-) \overset{def}{=} \frac{u_+}{u_-} = \frac{\rho_-}{\rho_+} = \frac{1}{\gamma+1}\left(\gamma + \frac{1}{{M_-}^2} - I\right), \tag{10a}$$

$$\psi(M_-) \overset{def}{=} \frac{{M_-}^2}{\gamma+1}\left(\gamma + \frac{1}{{M_-}^2} + \gamma I\right). \tag{10b}$$

By some simple calculations, we have

Theorem 2.2. $\phi'(M_-) > 0, \quad \psi'(M_-) < 0.$

Theorem 2.3. When $k < \frac{1}{\gamma^2-1}$, we have

$$\begin{aligned} M_* &= \sqrt{\frac{(\gamma-1)M_{**}^2+2}{2\gamma M_{**}^2-\gamma+1}}, \\ M_{**} &= \sqrt{\frac{(\gamma-1)M_*^2+2}{2\gamma M_*^2-\gamma+1}}. \end{aligned} \tag{11}$$

Proof. According to Lemma 2.1, M_* and M_{**} are the roots of the equation

$$\left(\gamma+\frac{1}{M^2}\right)^2 - 2(\gamma+1)\left(\frac{1}{M^2}+\frac{\gamma-1}{2}\right)(1+\kappa) = 0,$$

then we have

$$\begin{aligned} M_*^2 + M_{**}^2 &= \frac{2(\gamma+1)(\kappa+1)-2\gamma}{\gamma^2-(\gamma^2-1)(\kappa+1)}, \\ M_*^2 M_{**}^2 &= \frac{1}{\gamma^2-(\gamma^2-1)(\kappa+1)}. \end{aligned}$$

By solving the above equations, we can get (2.5). □

3 | STRUCTURE OF SOLUTION

Theorem 3.1. The exact solution of the Riemann problem (1.1)-(1.2) is self-similar, and consists of at most seven discontinuities. They are a heating discontinuity at $x = 0$, two genuinely nonlinear waves and a contact discontinuity left to $x = 0$, two genuinely nonlinear waves and a contact discontinuity right to $x = 0$ respectively, as shown in Figure 3.

Proof. We set

$$\tilde{U}(x,t) = U(\xi x, \xi t),$$

where ξ is a fixed number greater than 0. For any point(x,t) of $x \neq 0$, we have

$$\frac{\partial \tilde{U}(x,t)}{\partial t} + \frac{\partial F(\tilde{U}(x,t))}{\partial x} = \xi\left(\frac{\partial U(x,t)}{\partial t} + \frac{\partial F(U(x,t))}{\partial x}\right) = 0.$$

At the point (x,t) of $x = 0$, $\tilde{U}$ is a heating discontinuity and it satisfies the heat addition relation (1.3). Therefore $\tilde{U}$ is a solution of (1.1)-(1.2). Hence the exact solution of the Riemann problem (1.1)-(1.2) is self-similar.

From the above proof we know that $\tilde{U}(0-,t)$ and $\tilde{U}(0+,t)$ are constant vectors. The exact solution $U(x,t)$ in the left half $\{(x,t)|x < 0, t \geq 0\}$ satisfies the classical Euler equations, hence it is the left half of the CRP solution with U_1 and $U(0-,t)$ as the left and right initial conditions. From theory of the CRP solution, we know that $U(x,t)$ in the left half consists three discontinuities at most, which are two genuinely nonlinear waves, namely shock waves or rarefaction waves, and a contact discontinuity corresponding to the characteristic fields $u-a, u+a, a$ respectively, where a is the speed of sound. Similarly, $U(x,t)$ in the right half consists two genuinely nonlinear waves and a contact discontinuity at most. □

The elementary waves on the left and right sides are denoted as WL_1, WL_2, WL_3 and WR_1, WR_2, WR_3, respectively. The eight constant regions are labeled (1) $\sim$ (8), respectively. $U_1 \sim U_8$ are the states in regoins (1) $\sim$ (8) and it is obvious that $U_1 = U_8$. Note that the t-axis is a discontinuity and $U_4 \neq U_5$. We adopt similiar way to express the solution structure as in [15]. For examples, $S(U_1,U_2)$ and $R(U_1,U_2)$ mean two states U_1 and U_2 are connected by a shock and a rarefaction wave respectively, $C(U_2,U_3)$ means U_2 and U_3 are connected by a contact discontinuity, and $H(U_4,U_5)$ means U_4 and U_5 are connected by a heating discontinuity. The six elementary waves in Figure 3 can not exist at the same time. The next step in our double CRPs coupling method is to eliminate the redundant waves according to the heat addition properties and the gasdynamics properties. We will give the main results in Theorem 3.2 and then give the proof.

Theorem 3.2. According to the Mach number at the heating point, there are three different solution structures as follow:

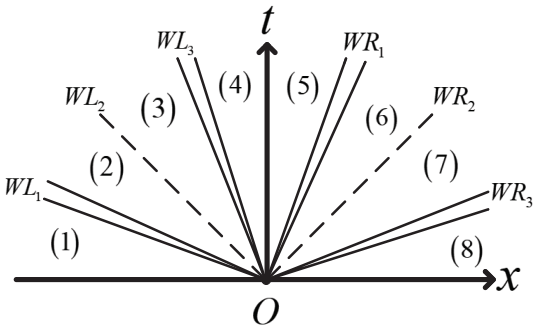

FIGURE 3 All possible waves for the Riemann problem (1.1)-(1.2)

(1) If $M_4 < M_5 < 1$, the wave pattern is

$$S(U_1, U_4) \oplus H(U_4, U_5) \oplus C(U_5, U_7) \oplus S(U_7, U_8);$$

(2) If $M_4 < M_5 = 1$, the wave pattern is

$$S(U_1, U_4) \oplus H(U_4, U_5) \oplus R(U_5, U_6) \oplus C(U_6, U_7) \oplus S(U_7, U_8);$$

(3) If $M_4 > M_5 \geq 1$, the wave pattern is

$$H(U_1, U_5) \oplus R(U_5, U_6) \oplus C(U_6, U_7) \oplus S(U_7, U_8).$$

Figure 4 depicts the three solution structures in the Theorem 3.2. They are called Structure 1, Structure 2 and Structure 3, respectively. According to the Mach number around the heating point and whether the thermal choking state appears, the proof of the Theorem 3.2 is divided into three parts, namely the following Lemma 3.1, Lemma 3.2 and Lemma 3.2, which corresponds to Structure 1, Structure 2 and Structure 3 respectively.

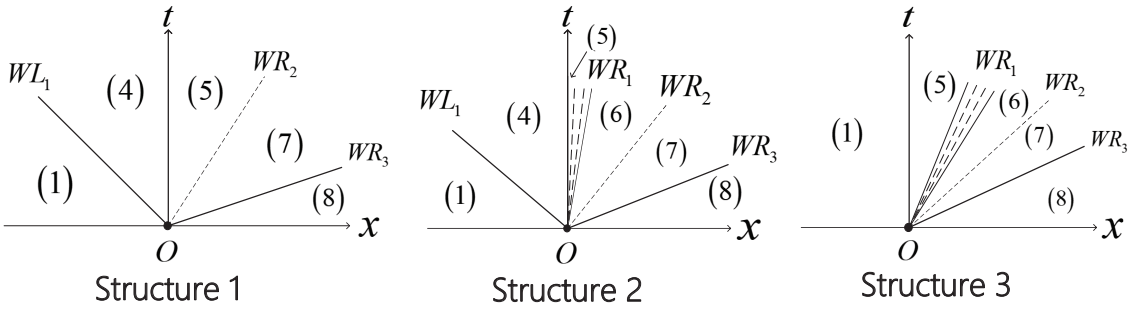

FIGURE 4 Three different solution structures

Lemma 3.1. When $M_4 < M_5 < 1$, WL_2, WL_3 and WR_1 do not exist, and $u_5 > u_4 > 0$ holds. If WL_1 and WR_3 exist, they are both shock waves.

Proof. u_4 and u_5 have the same sign according to (1.3a). WL_3 and WR_1 do not exist due to $M_4 < 1, M_5 < 1$. According to the sign of velocity at the heating point, there are three cases:

(1) If $u_4 > 0, u_5 > 0$, WL_2 does not exist;

(2) If $u_4 < 0, u_5 < 0$, WR_2 does not exist;

(3) If $u_4 = u_5 = 0$, WL_2 and WR_2 cling to the heating point and the widths of region 3 and region 6 are both zero.

These three structures are shown in Figure 5.

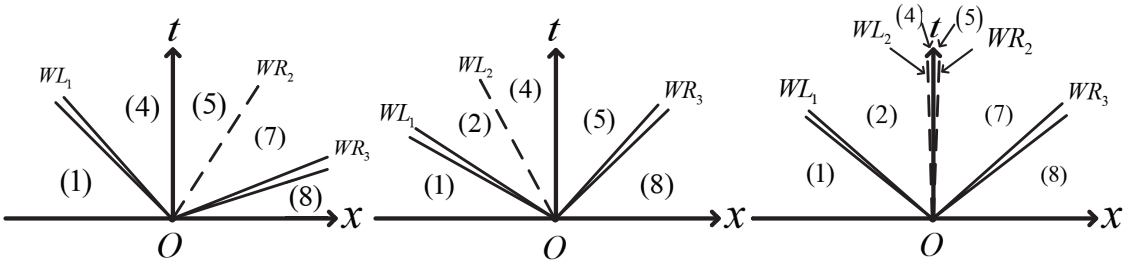

FIGURE 5 Three possible structures when subsonic flow is heated without thermal choke

If $u_4 < 0, u_5 < 0$, WL_1 is a shock wave and WR_3 is a rarefaction wave. $p_4 < p_5$ holds according to Theorem 2.1. The relation of elenmentary wave[21] implies that $p_1 \le p_2 = p_4$ and $p_5 \le p_8$. It results that $p_5 \le p_1$, which is contradictory with $p_5 > p_4 \ge p_1$, hence the structure of $u_4 < 0, u_5 < 0$ does not exist.

Using a similar method we can prove that the structure of $u_4 = u_5 = 0$ dose not exist. The structure of the solution is the same as the left image in Figure 5.

If WL_1 is a rarefaction wave, we have $p_7 = p_5 < p_4 \le p_1 = p_8$. Hence WR_3 is a rarefaction wave and $u_7 = u_5 > u_4 \ge u_1$ holds. Let us consider the control volume $[x_0, x_4] \times [0, T]$ in the $x - t$ space as shown in the left figure of Figure 6 and apply the conservation of mass and momentum. From $U_1 = U_8$, we have

$$\int_{x_0}^{x_4} \rho(x,T)dx = \int_{x_0}^{x_4} \rho(x,0)dx,$$
$$\int_{x_0}^{x_4} \rho(x,T)u(x,T)dx = \int_{x_0}^{x_4} \rho(x,0)u(x,0)dx.$$

The solution is constant in the each region, thus

$$\begin{aligned} &\int_{x_0}^{x_1} \rho(x,T)dx + \rho_4|x_1| + \rho_5|x_2| + \rho_7|x_3 - x_2| + \int_{x_3}^{x_4} \rho(x,T)dx \\ &= \int_{x_0}^{x_1} \rho(x,T)\frac{u(x,T)}{u_1}dx + \rho_4|x_1|\frac{u_4}{u_1} + \rho_5|x_2|\frac{u_5}{u_1} + \rho_7|x_3 - x_2|\frac{u_7}{u_1} + \int_{x_3}^{x_4} \rho(x,T)\frac{u(x,T)}{u_1}dx. \end{aligned} \tag{12}$$

Because the velocity inside the rarefaction wave is monotonous, we have $u(x,T) \ge max(u_1, u_4) \ge u_1$ for $x_0 \le x \le x_1$ and $u(x,T) \ge max(u_5, u_8) = u_5 > u_1$ for $x_3 \le x \le x_4$. Then we have

$$\int_{x_0}^{x_1} \rho(x,T)\frac{u(x,T)}{u_1}dx \ge \int_{x_0}^{x_1} \rho(x,T)dx.$$

$$\int_{x_3}^{x_4} \rho(x,T)\frac{u(x,T)}{u_1}dx \geq \int_{x_3}^{x_4} \rho(x,T)dx.$$

$\frac{u_4}{u_1} \geq 1$, $\frac{u_5}{u_1} > 1$ and $\frac{u_7}{u_1} > 1$ hold for the right side of (3.1). Therefore we have $x_2 = x_3 = 0$ and $u_5 = 0$, which are unreasonable. Thus WL_1 is a shock wave.

If WR_3 is a non-degenerate rarefaction wave, then $u_4 < u_5 = u_7 \leq u_8 = u_1$. Let us consider the control volume $[x_0, x_3]\times[0, T]$ in the $x - t$ space as shown in the right figure in Figure 6 and apply the conservation of mass and momentum. We have

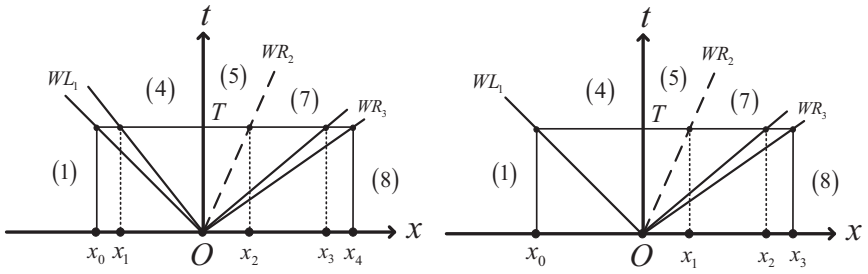

FIGURE 6 The integral diagram in the proof of Lemma 3.1. Left: assuming that WL_1 is a rarefaction wave and WR_3 is a rarefaction wave. Right: assuming that WL_1 is a shock wave and WR_3 is a rarefaction wave.

$$\int_{x_0}^{x_3} \rho(x,T)dx = \int_{x_0}^{x_3} \rho(x,0)dx,$$
$$\int_{x_0}^{x_3} \rho(x,T)u(x,T)dx = \int_{x_0}^{x_3} \rho(x,0)u(x,0)dx.$$

Thus

$$\begin{aligned}&\rho_4|x_0| + \rho_5|x_1| + \rho_7|x_2 - x_1| + \int_{x_2}^{x_3} \rho(x,T)dx \\ &= \rho_4|x_0|\frac{u_4}{u_1} + \rho_5|x_1|\frac{u_5}{u_1} + \rho_7|x_2 - x_1|\frac{u_7}{u_1} + \int_{x_2}^{x_3} \rho(x,T)\frac{u(x,T)}{u_1}dx.\end{aligned} \tag{13}$$

For the velocity u insides the rarefaction wave WR_3, we have $u(x,T) \leq max(u_5, u_8) = u_8 = u_1$. Then we have

$$\int_{x_2}^{x_3} \rho(x,T)\frac{u(x,T)}{u_1}dx \leq \int_{x_2}^{x_3} \rho(x,T)dx.$$

$\frac{u_4}{u_1} < 1$, $\frac{u_5}{u_1} \leq 1$ and $\frac{u_7}{u_1} \leq 1$ hold for the right side of (3.1). Therefore it hold that $\frac{u_7}{u_1} = 1$ and $U_7 = U_8$, which are unreasonable. Thus WR_3 is a shock wave. □

The following two lemmas can be proved using a similar method.

Lemma 3.2. When $M_4 < M_5 = 1$, WL_2 and WL_3 do not exist, and $u_5 > u_4 > 0$ holds. If WL_1, WR_1 and WR_3 exist, they are shock wave, rarefaction wave and shock wave, respectively.

Lemma 3.3. When $M_4 > M_5 \geq 1$, WL_1,WL_2 and WL_3 do not exist, and $u_5 > u_4 > 0$ holds. If WR_1 and WR_3 exist, they are rarefaction wave and shock wave, respectively.

For the rest of this paper, each wave and each constant region are marked the same as Figure 4.

Compared with Structure 1 and Structure 3, Structure 2 has one more wave, and the condition $M_5 = 1$ is used to match the number of conditions at this time.

4 | SOLUTION PROCEDURE

In this section, we will give procedures for solving the exact solution of each structure proposed in the third section.

For Structure 1 and Structure 2, the shock Mach number of WL_1 is

$$M_{SL} = \frac{s_L}{a_1},$$

where s_L is the velocity is WL_1. From the relation of the shock WL_1, we have

$$f_1(M_1, M_{SL}) \overset{def}{=} \frac{\rho_4}{\rho_1} = \frac{(\gamma+1)(M_1 - M_{SL})^2}{(\gamma-1)(M_1 - M_{SL})^2 + 2}, \tag{14a}$$

$$f_2(M_1, M_{SL}) \overset{def}{=} \frac{p_4}{p_1} = \frac{2\gamma(M_1 - M_{SL})^2 - \gamma + 1}{\gamma+1}, \tag{14b}$$

$$f_3(M_1, M_{SL}) \overset{def}{=} \frac{u_4 - s_L}{u_1 - s_L} = \frac{(\gamma-1)(M_1 - M_{SL})^2 + 2}{(\gamma+1)(M_1 - M_{SL})^2}. \tag{14c}$$

From (4.1c) we have

$$\begin{aligned} u_4 &= s_L + (u_1 - s_L) f_3(M_1, M_{SL}) \\ &= u_1 (f_3(M_1, M_{SL}) + \frac{s_L}{u_1}(1 - f_3(M_1, M_{SL}))) \\ &= u_1 (f_3(M_1, M_{SL}) + \frac{M_{SL}}{M_1}(1 - f_3(M_1, M_{SL}))) \end{aligned}$$

and

$$a_4 = a_1 \sqrt{\frac{f_2(M_1, M_{SL})}{f_1(M_1, M_{SL})}}.$$

We set

$$f_4(M_1, M_{SL}) \overset{def}{=} \frac{u_4}{u_1} = f_3(M_1, M_{SL}) + \frac{M_{SL}}{M_1}(1 - f_3(M_1, M_{SL})). \tag{15}$$

The relation between Mach Numbers is

$$\begin{aligned} M_4 = \frac{u_4}{a_4} &= M_1 f_4(M_1, M_{SL}) \sqrt{\frac{f_1(M_1, M_{SL})}{f_2(M_1, M_{SL})}} \\ &= \frac{((\gamma-1)M_1 + 2M_{SL})(M_1 - M_{SL}) + 2}{\sqrt{2\gamma(M_1 - M_{SL})^2 - \gamma + 1}\sqrt{(\gamma-1)(M_1 - M_{SL})^2 + 2}} \\ &= \frac{((\gamma-1)M_1 + 2M_{SL})(M_1 - M_{SL}) + 2}{\sqrt{2\gamma(\gamma-1)(M_1 - M_{SL})^4 + (6\gamma - \gamma^2 - 1)(M_1 - M_{SL})^2 - 2(\gamma-1)}}. \end{aligned} \tag{16}$$

We set

$$f_5(M_1, M_{SL}) \overset{def}{=} \frac{((\gamma-1)M_1 + 2M_{SL})(M_1 - M_{SL}) + 2}{\sqrt{2\gamma(\gamma-1)(M_1 - M_{SL})^4 + (6\gamma - \gamma^2 - 1)(M_1 - M_{SL})^2 - 2(\gamma-1)}}. \tag{17}$$

From (2.4), we have

$$\frac{p_5}{p_4} = \psi(M_4) = \psi(f_5(M_1, M_{SL})), \tag{18a}$$

$$\frac{u_5}{u_4} = \phi(M_4) = \phi(f_5(M_1, M_{SL})). \tag{18b}$$

It is obtained from the shock relation of WR_3 that

$$u_5 - u_8 = \sqrt{\frac{\beta p_8}{\rho_8}} \frac{p_5/p_8 - 1}{\sqrt{1 + \tau p_5/p_8}}$$

where $\beta = 2/(\gamma - 1), \tau = (\gamma + 1)/(\gamma - 1)$.

Substituting (4.1), (4.2) and (4.5) into the above equation, we get

$$M_1(f_4(M_1, M_{SL})\phi(M_4) - 1) - \sqrt{\frac{\beta}{\gamma}} \frac{f_2(M_1, M_{SL})\psi(M_4) - 1}{\sqrt{1 + \tau f_2(M_1, M_{SL})\psi(M_4)}} = 0. \tag{19}$$

(4.3) and (4.6) form a system of equations for M_{SL} and M_4 as follows:

$$\begin{cases} M_1(f_4(M_1, M_{SL})\phi(M_4) - 1) - \sqrt{\frac{\beta}{\gamma}} \frac{f_2(M_1, M_{SL})\psi(M_4) - 1}{\sqrt{1 + \tau f_2(M_1, M_{SL})\psi(M_4)}} = 0 \\ M4 = \frac{((\gamma - 1)M_1 + 2M_{SL})(M_1 - M_{SL}) + 2}{\sqrt{2\gamma(\gamma - 1)(M_1 - M_{SL})^4 + (6\gamma - \gamma^2 - 1)(M_1 - M_{SL})^2 - 2(\gamma - 1)}} \end{cases} \tag{20}$$

From the entropy condition of the shock wave[22], we have

$$M_1 - M_{SL} = \frac{u_1}{a_1} - \frac{s_L}{a_1} \geq 1. \tag{21}$$

Theorem 4.1. If M_1 and M_4 are taken as known quantities, the M_{SL} which satisfies (4.3) and (4.8) exists and is unique.

Proof. (4.3) has another form:

$$\begin{aligned} &M_4\sqrt{(\gamma - 1)(M_1 - M_{SL})^2 + 2}\sqrt{2\gamma(M_1 - M_{SL})^2 - \gamma + 1} \\ =& -2(M_1 - M_{SL})^2 + (\gamma + 1)M_1(M_1 - M_{SL}) + 2. \end{aligned}$$

We divide both sides of the above equation by $M_1 - M_{SL}$ and get

$$\begin{aligned} &M_4\sqrt{(\gamma - 1)(M_1 - M_{SL})^2 + 2}\sqrt{2\gamma - \frac{\gamma + 1}{(M_1 - M_{SL})^2}} \\ =& -2(M_1 - M_{SL}) + (\gamma + 1)M_1(M_1 - M_{SL}) + \frac{2}{(M_1 - M_{SL})^2}. \end{aligned}$$

We set

$$\begin{aligned} \sigma_1(x) &\overset{def}{=} M_4\sqrt{(\gamma - 1)x^2 + 2}\sqrt{2\gamma - \frac{\gamma + 1}{x^2}}, \\ \sigma_2(x) &\overset{def}{=} 2x - (\gamma + 1)M_1 - \frac{2}{x}, \\ \sigma(x) &\overset{def}{=} \sigma_1(x) + \sigma_2(x). \end{aligned}$$

The domains of $\sigma_1(x)$, $\sigma_2(x)$ and $\sigma(x)$ are $\{x|x \geq 1\}$. Both $\sigma_1(x)$ and $\sigma_2(x)$ are monotone increasing functions, hence $\sigma(x)$ is a monotone increasing function. We have

$$\begin{aligned} \sigma(1) &= (\gamma + 1)(M_4 - M_1) \leq 0, \\ \lim_{x\to\infty} \sigma(x) &= \lim_{x\to\infty} \sigma_1(x) + \lim_{x\to\infty} \sigma_2(x) = \infty. \end{aligned}$$

Therefore the root of $\sigma(x)$ exists and is unique in the domain.

$M_1 - M_{SL}$ is the root of $\sigma(x)$. Therefore, the M_{SL} that satisfies (4.3) and entropy condition (4.8) exists and is unique. □

The procedure for accessing the exact solution of Structure 1 is as follows:

Step1: Iteratively solve (4.7) for M_{SL}, then get M_4 using (4.3);

Step2: Evaluate $\rho_4/\rho_1, p_4/p_1, u_4/u_1$ and s_L by (4.1), then U_4 can be obtained;

Step3: Evaluate U_5 by (2.1);

Step4: Evaluate U_7 by a solver of CRP.

According to Theorem 4.1, the solution of M_{SL} in the Step 1 is unique. It should be noted that M_4 and M_5 are only related to M_1, thus there is an equivalence between the range of M_1 and the assumption that the heating flow is subsonic and no thermal choke appears. Besides, the ratios of the variables in region 4, region 5 and region 7 to the corresponding variables of the initial state are also only related to M_1.

For Structure 2, we have

$$M_* = \frac{((\gamma-1)M_1 + 2M_{SL})(M_1 - M_{SL}) + 2}{\sqrt{2\gamma(\gamma-1)(M_1 - M_{SL})^4 + (6\gamma - \gamma^2 - 1)(M_1 - M_{SL})^2 - 2(\gamma-1)}}. \tag{22}$$

Thus we can solve the left and right half parts of the exact solution separately for Structure 2. The procedure for accessing the exact solution of Structure 2 is as follows:

Step1: Iteratively solve (4.9) for M_{SL};

Step2: Evaluate $\rho_4/\rho_1, p_4/p_1, u_4/u_1$ and s_L by (4.1);

Step3: Evaluate U_5 by (2.1);

Step4: Evaluate U_6 and U_7 by a solver of CRP with U_5 and U_8 as the left and right initial states.

According to Theorem 4.1, the solution of M_{SL} in the Step 1 is unique.

For Structure 3, the incoming flow is directly heated. The solution precudure is much simpler, as shown below:

Step1: Evaluate U_5 by (2.2);

Step2: Evaluate U_6 and U_7 by a solver of CRP with U_5 and U_8 as the left and right initial states.

For the Step 4 in the solution precedure of Structure 1, Structure 2 and the Step 2 in the solution precudure of Structure 3, a CRP solver of Euler equations is needed. For the solutions of these CRPs, the wave patterns are identical, which consists a rarefaction wave corresponding to the $u - a$ characteristic field and a shock wave corresponding to the $u + a$ charatristic field.

We describe the strength of each nonlinear wave in terms of the ratio of pressures on both sides of the wave. Then the following theorem holds:

Theorem 4.2. It holds for each solution structure: the strength of each nonlinear wave is determined by the Mach number of the initial condition, independent of other variables of the initial condition.

Proof. For Structure 1, (4.1) and (4.5) imply

$$\begin{aligned} &p_4/p_1 = f_2(M_1, M_{SL}), \\ &p_8/p_7 = p_1/p_4 \times p_4/p_5 = \left[f_2(M_1, M_{SL}\psi(f_5(M_1, M_{SL})))\right]^{-1}, \end{aligned} \tag{23}$$

where M_{SL} is obtained from equation (4.7) and is determined by M_1.

For Structure 2, we have:

$$p_4/p_1 = f_2(M_1, M_{SL}),$$

where M_{SL} is obtained from equation (4.9) and is determined by M_1.

From the elementary wave equation[27], we get:

$$\begin{aligned} u_6 &= u_5 - \frac{2a_5}{\gamma-1}\left[\left(\frac{p_6}{p_5}\right)^{\frac{\gamma-1}{2\gamma}} - 1\right], \\ u_7 &= u_8 + \sqrt{2}(p_7 - p_8)\left[(\gamma+1)p_7\rho_8 + (\gamma-1)p_8\rho_8\right]^{-\frac{1}{2}}. \end{aligned} \tag{24}$$

According to $u_6 = u_7$, $p_6 = p_7$ and $U_1 = U_8$, we have

$$u_5 - \frac{2a_5}{\gamma - 1}\left[\left(\frac{p_6}{p_5}\right)^{\frac{\gamma-1}{2\gamma}} - 1\right] = u_1 + \sqrt{2}(p_6 - p_1)\left[(\gamma+1)p_6\rho_1 + (\gamma-1)p_1\rho_1\right]^{-\frac{1}{2}}. \tag{25}$$

Divide both sides of the equation (4.12) by a_1, then

$$\frac{u_5}{u_1}M_1 - \frac{2}{\gamma-1}\frac{M_1}{M_5}\frac{u_5}{u_1}\left[\left(\frac{p_6}{p_5}\right)^{\frac{\gamma-1}{2\gamma}} - 1\right] = M_1 + \frac{\sqrt{2}}{a_1}(p_6 - p_1)\left[(\gamma+1)p_6\rho_1 + (\gamma-1)p_1\rho_1\right]^{-\frac{1}{2}}. \tag{26}$$

Apply the equation of state to (4.13), we have

$$\frac{u_5}{u_1}M_1 - \frac{2}{\gamma-1}\frac{M_1}{M_5}\frac{u_5}{u_1}\left[\left(\frac{p_6}{p_5}\right)^{\frac{\gamma-1}{2\gamma}} - 1\right] = M_1 + \sqrt{\frac{2}{\gamma}}(\frac{p_6}{p_1} - 1)\left[(\gamma+1)\frac{p_6}{p_1} + (\gamma-1)\right]^{-\frac{1}{2}}. \tag{27}$$

Therefore p_6/p_5 satisfies the following equation:

$$\left(A\left(\frac{p_6}{p_5}\right)^{\frac{\gamma-1}{2\gamma}} + B\right)\sqrt{C\frac{p_6}{p_5} + \gamma - 1} - \sqrt{\frac{2}{\gamma}}\left(\frac{C}{\gamma+1}\frac{p_6}{p_5} - 1\right) = 0, \tag{28}$$

where $A = -\frac{2}{\gamma-1}M_1\phi(M_*)f_4(M_1, M_{SL})$, $B = \frac{\gamma+1}{\gamma-1}M_1\phi(M_*)f_4(M_1, M_{SL})$, $C = (\gamma+1)\psi(M_*)f_2(M_1, M_{SL})$ and M_{SL} is obtained form equation (4.9). Thus the strength of WR_1 in Structure 2 is determined by M_1.

For WR_3, we have

$$\frac{p_8}{p_7} = \left[f_2(M_1, M_{SL})\psi(M_*)\frac{p_6}{p_5}\right]^{-1}.$$

Therefore the strength of each nonlinear wave in Structure 2 is determined by M_1.

The analysis method of Structure 3 is similar to the analysis method of Structure 2. We have

$$\begin{aligned}&\left(A'\left(\frac{p_6}{p_5}\right)^{\frac{\gamma-1}{2\gamma}} + B'\right)\sqrt{C'\frac{p_6}{p_5} + \gamma - 1} - \sqrt{\frac{2}{\gamma}}\left(\frac{C'}{\gamma+1}\frac{p_6}{p_5} - 1\right) = 0,\\ &\frac{p_8}{p_7} = \left[\frac{p_5}{p_1}\frac{p_6}{p_5}\right]^{-1},\end{aligned} \tag{29}$$

where $A' = -\frac{2}{\gamma-1}\frac{M_1}{M_5}\frac{u_5}{u_1}$, $B' = \frac{u_5}{u_1}M_1 + \frac{2}{\gamma-1}\frac{M_1}{M_5}\frac{u_5}{u_1}$, $C' = (\gamma+1)\frac{p_5}{p_1}$. $\frac{u_5}{u_1}$, $\frac{p_5}{p_1}$ and M_5 in (4.16) is obtained from (3.1) and they are all detrmined by M_1. □

5 | UNIQUENESS OF SOLUTION

In this section we will study the reasonable range of M_1 for the three structures of the exact sulution. The other contribution of this work is to obtain the uniqueness of the solution. In addition, the determination of M_1 to the structure of the solution helps to reduce the computational cost.

For Structure 1 and Structure 2, the following equation holds:

$$M_4 = \frac{((\gamma-1)M_1 + 2M_{SL})(M_1 - M_{SL}) + 2}{\sqrt{2\gamma(\gamma-1)(M_1 - M_{SL})^4 + (6\gamma - \gamma^2 - 1)(M_1 - M_{SL})^2 - 2(\gamma-1)}}.$$

From the above equation we can get

$$A(M_1 - M_{SL})^4 + B(M_1 - M_{SL})^3 + C(M_1 - M_{SL})^2 + D(M_1 - M_{SL}) + E = 0, \tag{30}$$

where

$$A = 4 - 2\gamma(\gamma - 1)M_4^2,$$
$$B = -4(\gamma + 1)M_1,$$
$$C = (\gamma + 1)^2 M_1^2 - 8 - (6\gamma - \gamma^2 - 1)M_4^2,$$
$$D = 4(\gamma + 1)M_1,$$
$$E = 4 + 2(\gamma - 1)M_4^2.$$

$M_1 - M_{SL}$ is the root of equation (5.1). According to Theromen 4.1, the entropy solution of (5.1) is unique, which is a smooth function of M_1 and M_{SL} defined as follows:

$$M_{SL} = f_6(M_1, M_4).$$

We set

$$X(M_1, M_4) \overset{def}{=} M_1(f_4(M_1, M_{SL})\phi(M_4) - 1) - \sqrt{\frac{\beta}{\gamma}} \frac{f_2(M_1, M_{SL})\psi(M_4) - 1}{\sqrt{1 + \tau f_2(M_1, M_{SL})\psi(M_4)}}, \tag{31}$$

$$Y(M_1) \overset{def}{=} X(M_1, M_*), \tag{32}$$

where $M_{SL} = f_6(M_1, M_4)$.

Lemma 5.1. For the solution of Structure 1, $Y(M_1) \geq 0$ holds.

Proof. From (4.6), we know that

$$X(M_1, M_4) = 0.$$

It can be proved that

$$\frac{\partial f_5}{\partial M_{SL}} > 0$$

and

$$\frac{\partial f_6}{\partial M_{SL}} = \left(\frac{\partial f_5}{\partial M_{SL}}\right)^{-1} > 0.$$

Then we have

$$\frac{\partial X}{\partial M_4} = M_1 \frac{\partial}{\partial M_4}(f_4(M_1, M_{SL})\phi(M_4)) - \sqrt{\frac{\beta}{\gamma}} \frac{\partial}{\partial M_4}\left(\frac{f_2(M_1, M_{SL})\psi(M_4) - 1}{\sqrt{1 + \tau f_2(M_1, M_{SL})\psi(M_4)}}\right). \tag{33}$$

For the first part on the right of (5.4), we have

$$\frac{\partial}{\partial M_4}(f_4(M_1, M_{SL})\phi(M_4)) = \frac{\partial f_4(M_1, M_4)}{\partial M_4}\phi(M_4) + \frac{d\phi(M_4)}{dM_4} f_4(M_1, M_{SL}),$$
$$\frac{\partial f_4(M_1, M_4)}{\partial M_4} = \frac{\partial f_4(M_1, M_4)}{\partial M_{SL}} \frac{\partial M_{SL}}{\partial M_4} = \frac{2(1 + (M_1 - M_{SL})^{-2})}{(\gamma + 1)M_1} \frac{\partial f_6}{\partial M_4} > 0,$$
$$\phi'(M_4) > 0.$$

Thus we have proved that

$$\frac{\partial}{\partial M_4}(f_4(M_1, M_{SL})\phi(M_4)) > 0.$$

For the second part on the right of (5.4), we have

$$\frac{\partial}{\partial M_4}\left(\frac{f_2(M_1, M_{SL})\psi(M_4) - 1}{\sqrt{1 + \tau f_2(M_1, M_{SL})\psi(M_4)}}\right) = \frac{\tau(f_2(M_1, M_{SL})\psi(M_4) + 1) + 2}{2(f_2(M_1, M_{SL})\psi(M_4))^{3/2}} \frac{\partial}{\partial M_4}(f_2(M_1, M_{SL})\psi(M_4)),$$
$$\frac{\partial}{\partial M_4}(f_2(M_1, M_{SL})\psi(M_4)) = -\left(\frac{\partial f_2}{\partial M_1} - \frac{\partial f_2}{\partial M_{SL}}\right)\psi(M_4) + \frac{d\psi(M_4)}{dM_{SL}} f_2(M_1, M_{SL}),$$
$$\frac{\partial f_2}{\partial M_1} - \frac{\partial f_2}{\partial M_{SL}} > 0,$$
$$\psi'(M_4) < 0.$$

Thus we have

$$\frac{\partial}{\partial M_4}(f_2(M_1, M_{SL})\psi(M_4)) < 0$$

and

$$\frac{\partial}{\partial M_4}\left(\frac{f_2(M_1,M_{SL})g_2(M_1,M_{SL})-1}{\sqrt{1+\tau f_2(M_1,M_{SL})g_2(M_1,M_{SL})}}\right)<0.$$

From the above equations, we have

$$\frac{\partial X}{\partial M_4}>0.$$

From Lemma 2.1 we know that $M_4 < M_*$, thus

$$Y(M_1)=X(M_1,M_*)\geq X(M_1,M_4)=0.$$

□

Lemma 5.2. $Y(M_1)\leq 0$ and $M_1 \leq M_{**}$ (if M_{**} exists) are two necessary conditions for Structure 2.

Proof. The solution right to $x = 0$ in Structure 2 is the solution of a CRP, whose wave pattern is $R(U_5,U_6)\oplus C(U_6,U_7)\oplus S(U_7,U_8)$, then the following equation holds[23]:

$$u_5-u_8\leq\sqrt{\frac{\beta p_8}{\rho_8}}\frac{p_5/p_8-1}{\sqrt{1+\tau p_5/p_8}}.$$

The above equation can be transformed into

$$M_1(f_4(M_1,M_{SL})\phi(M_*)-1)-\sqrt{\frac{\beta}{\gamma}}\frac{f_2(M_1,M_{SL})\psi(M_*)-1}{\sqrt{1+\tau f_2(M_1,M_{SL})\psi(M_*)}}\leq 0.$$

Thus we have

$$Y(M_1)\leq 0. \tag{34}$$

For structure 2, we set

$$M'_{SL}=\frac{s_L}{a_4},$$

where s_L is the velocity of WL_1 and a_4 is the speed of sound in region 4.

Similar to (4.3), the following equation holds:

$$M_1=\frac{((\gamma-1)M_4+2M'_{SL})(M_4-M'_{SL})+2}{\sqrt{2\gamma(\gamma-1)(M_4-M'_{SL})^4+(6\gamma-\gamma^2-1)(M_4-M'_{SL})^2-2(\gamma-1)}}.$$

We set

$$g(M_4,M'_{SL})=\frac{((\gamma-1)M_4+2M'_{SL})(M_4-M'_{SL})+2}{\sqrt{2\gamma(M_4-M'_{SL})^2-\gamma+1}\sqrt{(\gamma-1)(M_4-M'_{SL})^2+2}}.$$

The domain of g satisfies

$$M_4\leq M_*,\quad M'_{SL}\leq 0.$$

It can be proved that

$$\frac{\partial g}{\partial M'_{SL}}>0.$$

Thus we have

$$g(M_4,M'_{SL})\leq g(M_4,0)=\sqrt{\frac{(\gamma-1)M_4^2+2}{2\gamma M_4^2-\gamma+1}}$$

and

$$M_1=g(M_*,M'_{SL})\leq g(M_*,0)=\sqrt{\frac{(\gamma-1)M_*^2+2}{2\gamma M_*^2-\gamma+1}}.$$

According to Theorem 2.3, we have

$$M_{**}=\sqrt{\frac{(\gamma-1)M_*^2+2}{2\gamma M_*^2-\gamma+1}}.$$

Therefore we have proved that

$$M_1\leq M_{**}.$$

□

The following lemma can be derived directly by Lemma 2.1:

Lemma 5.3. When $k < \frac{1}{\gamma^2-1}$, a necessary condition for the solution of Structure 3 is $M_1 \geq M_{**}$. When $k \geq \frac{1}{\gamma^2-1}$, the solution of Structure 3 does not exists.

When $k \geq \frac{1}{\gamma^2-1}$, M_{**} does not exist. Therefore, the upstream flow of the heating point must be a subsonic flow. At this time, there are only two structures: Structure 1 and Structure 2. No matter what the Mach number of the incoming flow is, it drops below 1 after passing through the upward shock wave. When $K < \frac{1}{\gamma^2-1}$, all three structures are possible. According to Lemma 5.1, Lemma 5.2 and Lemma 5.3, the following conclusions hold:

Theorem 5.1. When $k \geq \frac{1}{\gamma^2-1}$, the solution can only have two structures: Strcture 1 and Structure 2. When $k < \frac{1}{\gamma^2-1}$, all three structures are possible. For the three solution structures, there are the following necessary conditions:

(1) For Structure 1, $Y(M_1) \geq 0$ holds;

(2) For Structure 2, $Y(M_1) \leq 0$ and $M_* \leq M_1 \leq M_{**}$ hold;

(3) For Structure 3, $M_1 \geq M_{**}$ holds.

From Theorem 5.1 we can directly obtain the following conclusions:

Theorem 5.2. (a) When $k \geq \frac{1}{\gamma^2-1}$, the solution of Riemann problem (1.1)-(1.2) is unique.

(b) When $k < \frac{1}{\gamma^2-1}$, The solution of Riemann problem (1.1)-(1.2) is unique under the assumption that the root of $Y(M_1)$ is not greater than M_{**}.

It can be seen from Theorem 5.1 that the structure of M_1 equaling to the root of $Y(M_1)$ is the demarcation structure of Structure 1 and Structure 2, whose wave pattern is

$$S(U_1, U_4) \oplus H(U_4, U_5) \oplus C(U_5, U_7) \oplus S(U_7, U_8) \quad \text{with} \quad M_4 = M_*.$$

And the structure of M_1 equaling to M_{**} is the demarcation structure of Structure 2 and Structure 3, whose wave pattern is

$$S(U_1, U_4) \oplus H(U_4, U_5) \oplus R(U_5, U_6) \oplus C(U_6, U_7) \oplus S(U_7, U_8) \quad \text{with} \quad s_L = 0, \tag{35}$$

or

$$H(U_1, U_5) \oplus R(U_5, U_6) \oplus C(U_6, U_7) \oplus S(U_7, U_8) \quad \text{with} \quad M_5 = 1. \tag{36}$$

Remark 1. The structure of (5.6) is a limit structure of Structure 2. WL_1 is a normal shock and $M_4 = M_*$ hold at this time, which imply that $M_1 = M_{**}$. For the structure of (5.7), $M_5 = 1$ implies that $M_1 = M_{**}$. Therefore the structure of (5.6) equals to the structure of (5.7).

For the case that the root of $Y(M_1)$ is greater than M_{**}, the uniqueness of the solution has not been proved. To compare the size of the root of $Y(M1)$ and M_{**}, we set

$$R(\gamma, k) = \textit{the root of } Y,$$
$$T(\gamma, k) = M_{**} - R(\gamma, k).$$

In Figure 7 we show the contour map of the function T. The curved boundary on the upper right is the curve of $k = \frac{1}{\gamma^2-1}$. From Figure 7 we can see that $T(\gamma, k)$ is greater than 0, therefore the root of $Y(M_1)$ is smaller than M_{**} and the assumption in the second part of Theorem 5.2 is always holds. We give the following conjecture:

Conjecture 5.1. The solution of Riemann problem (1.1)-(1.2) is always unique for any γ and any κ. The structure of the solution is determined by M_1, as shown below:

(1) if M_1 is less than the root of Y, the wave pattern is Structure 1;

(2) if M_1 is greater than the root of Y and less than M_{**}, the wave pattern is Structure 2;

(3) if M_1 is greater than M_{**}, the wave pattern is Structure 3.

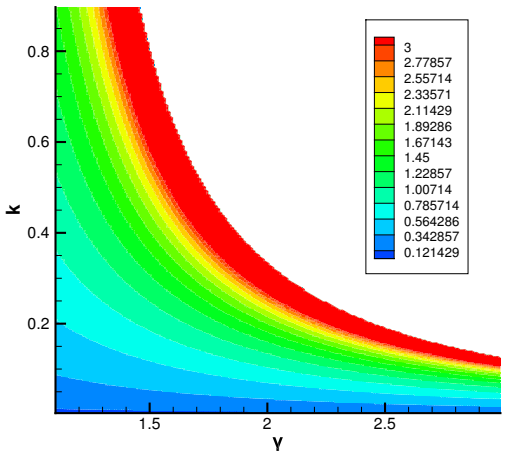

FIGURE 7 The contour map of function $T(\gamma, k)$

6 | VERIFICATION

In this section, we will construct five examples with $\gamma = 1.4$. In the first four examples, we take the heating coefficient $k = 0.2$, then $k < \frac{1}{\gamma^2-1}$ holds. M_* and M_{**} are 0.6136 and 1.8130 respectively. The root of $Y(M_1)$ is 1.0620, which is less than M_{**}, hence the solution is unique. These four examples contain the solutions of Structure 1, Structure 2 and Structure 3. In the last example, the value of k is 2.0. $k > \frac{1}{\gamma^2-1}$ holds at this time. From Theorem 5.2 we know that the solution is unique. The wave pattern of the example is Structure 2.

We first gives two exact solutions of Structure 1. The initial conditions are $(\rho_1, u_1, p_1) = (1.0, 0.8, 1.0)$ and $(\rho_1, u_1, p_1) = (1.0, 1.2, 1.0)$ respectively and their exact solutions are shown in Figure 8 and Figure 9.

The third example has an exact solution of Structure 2. The initial condition is $(\rho_1, u_1, p_1) = (1.0, 1.8, 1.0)$. The states of each region are shown in Figure 10.

The fourth example has an exact solution of Structure 3. The initial condition is $(\rho_1, u_1, p_1) = (1.0, 2.8, 1.0)$. The states of each region are shown in Figure 11.

The fifth example has an exact solution of Structure 2. The initial condition is $(\rho_1, u_1, p_1) = (1.0, 2.8, 1.0)$. The states of each region are shown in Figure 12.

7 | CONCLUSIONS

This paper focused on the Riemann problem of the Euler equations with a Dirac delta-source in the energy conservation eqution. We proved that there are three structures of the solution and proposed an iterative method of the exact solution. In addition, we associated each structure of the solution with the Mach number of the initial condition, thereby obtained some conclusions about the uniqueness of solution.

The present method is completely different from the existing method of dealing with the Riemann problem with discontinuous source. Based on CRP solution structures, the strategy of the present method is the elimination of unconscionable waves on the general structure (Figure 3). This method can be applied to the Riemann problem of other hyperbolic systems with Dirac

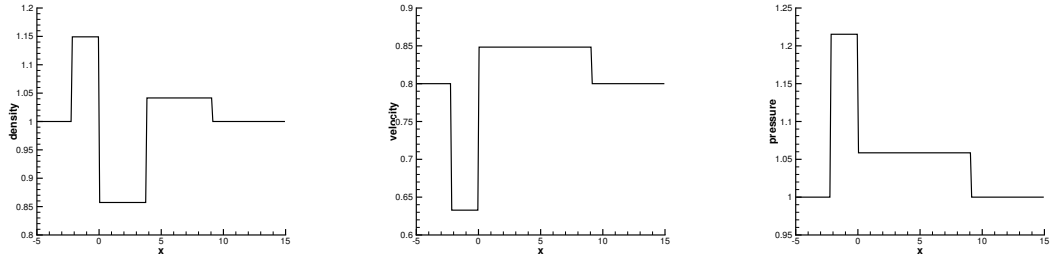

(a) density (b) velocity (c) pressure

FIGURE 8 The exact solution of $t = 4.5s$ with initial condition $(\rho_1, u_1, p_1) = (1.0, 0.8, 1.0)$ and $k = 0.2$

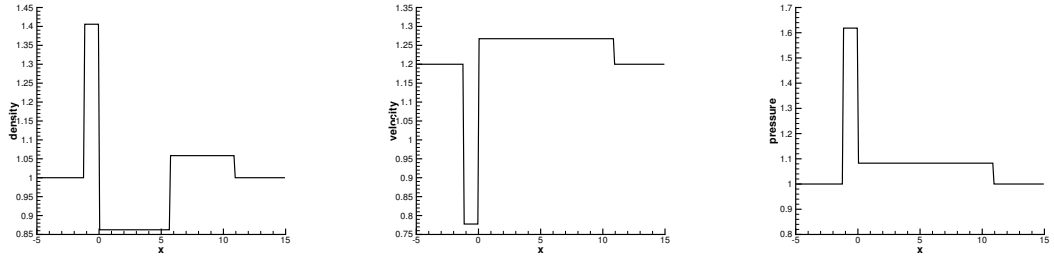

(a) density (b) velocity (c) pressure

FIGURE 9 The exact solution of $t = 4.5s$ with initial condition $(\rho_1, u_1, p_1) = (1.0, 1.2, 1.0)$ and $k = 0.2$

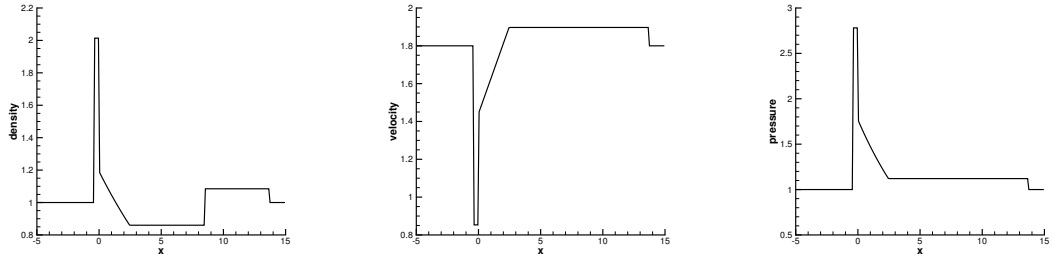

(a) density (b) velocity (c) pressure

FIGURE 10 The exact solution of $t = 4.5s$ with initial condition $(\rho_1, u_1, p_1) = (1.0, 1.8, 1.0)$ and $k = 0.2$

delta-function sources or other sources. Compared with the method of augmented equations, it is more simple and can naturally cover all possible structures.

Such heating problem (Figure 1) can be seen in man-made channels and natural streams, such as condensation probelm. The results of this paper provide theoretical support for the study of some condensation phenomena. The exact solution of the Riemann problem can be directly applied to the flux calculation of Godunov-type methods[24] in numerical simulation. The exact solutions constructed by this method, such as the examples in the sixth section, can be used to evaluate the existing numerical methods of dealing with source terms, such as[25,26,13]. In addition, this work has potential in the area of interface processing for multi-phase flow simulation with the Riemann problem based interface algorithms. The uniqueness of solutions under arbitrary

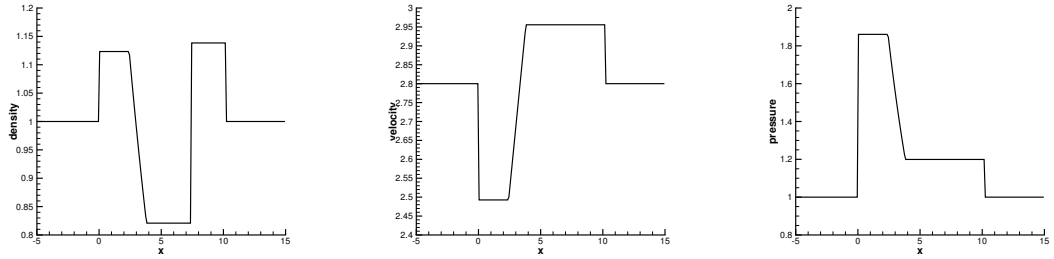

(a) density (b) velocity (c) pressure

FIGURE 11 The exact solution of $t = 2.5s$ with initial condition $(\rho_1, u_1, p_1) = (1.0, 2.8, 1.0)$ and $k = 0.2$

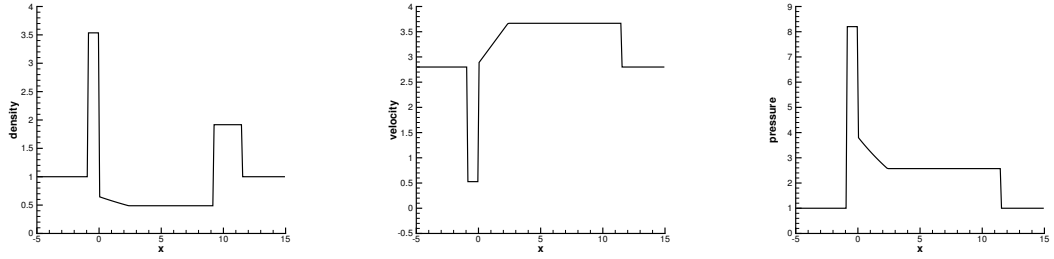

(a) density (b) velocity (c) pressure

FIGURE 12 The exact solution of $t = 2.5s$ with initial condition $(\rho_1, u_1, p_1) = (1.0, 2.8, 1.0)$ and $k = 2.0$

initial conditions is an unsolved problem, which is the goal of our future work. In addition, future work should focus on the heating addition of unsteady flow, in which the transition of the three structures proposed in this paper may occur.

References

1. Delale Can F., Schnerr Günter H., Dongen Marinus E. H. Van. *Condensation Discontinuities and Condensation Induced Shock Waves*. 2007.

2. Dongen M. E. H. Van, Luo X., Lamanna G., Kaathoven D. J. Van. On Condensation Induced Shock Waves. In: ; 2002.

3. Delale Can F, Schnerr G H, Zierep Jurgen. The mathematical theory of thermal choking in nozzle flows. *Zeitschrift für Angewandte Mathematik und Physik*. 1993;44(6):943–976.

4. Schnerr Gunter. Unsteadiness in Condensing Flow: Dynamics of Internal Flows with Phase Transition and Application to Turbomachinery. *Journal of Mechanical Engineering Science*. 2005;219.

5. Cheng Wan, Luo Xisheng, Dongen Van Meh Rini. On condensation-induced waves. *Journal of Fluid Mechanics*. 2010;651(1):145–164.

6. Luo Xisheng, Prast B Bart, Dongen Van Meh Rini, Hoeijmakers Hwm Harrie, Yang J. On phase transition in compressible flows: modelling and validation. *Journal of Fluid Mechanics*. 2006;548(1):403–430.

7. Benartzi Matania, Falcovitz Joseph. A second-order Godunov-type scheme for compressible fluid dynamics. *Journal of Computational Physics*. 1984;55(1):1–32.

8. Benartzi Matania, Li Jiequan, Warnecke Gerald. A direct Eulerian GRP scheme for compressible fluid flows. *Journal of Computational Physics.* 2006;218(1):19–43.

9. Toro Eleuterio F, Hidalgo Arturo. ADER finite volume schemes for nonlinear reaction–diffusion equations. *Applied Numerical Mathematics.* 2009;59(1):73–100.

10. Toro Eleuterio F, Montecinos Gino I. Implicit, semi-analytical solution of the generalized Riemann problem for stiff hyperbolic balance laws. *Journal of Computational Physics.* 2015;303:146–172.

11. Li Jiequan, Chen Guoxian. The generalized Riemann problem method for the shallow water equations with bottom topography. *International Journal for Numerical Methods in Engineering.* 2006;65(6):834–862.

12. Li Jiequan, Liu Tiegang, Sun Zhongfeng. Implementation of the GRP scheme for computing radially symmetric compressible fluid flows. *Journal of Computational Physics.* 2009;228(16):5867–5887.

13. Kroner Dietmar, Thanh Mai Duc. Numerical Solutions to Compressible Flows in a Nozzle with Variable Cross-section. *SIAM Journal on Numerical Analysis.* 2005;43(2):796–824.

14. Lefloch Philippe G, Thanh Mai Duc. The Riemann Problem for Fluid Flows in a Nozzle with Discontinuous Cross-Section. *Communications in Mathematical Sciences.* 2003;1(4):763–797.

15. Thanh Mai Duc. The Riemann Problem for a Nonisentropic Fluid in a Nozzle with Discontinuous Cross-Sectional Area. *Siam Journal on Applied Mathematics.* 2009;69(6):1501–1519.

16. Alcrudo Francisco, Benkhaldoun Fayssal. Exact solutions to the Riemann problem of the shallow water equations with a bottom step. *Computers & Fluids.* 2001;30(6):643 - 671.

17. Bernetti R, Titarev V A, Toro Eleuterio F. Exact Solution of the Riemann Problem for the Shallow Water Equations with Discontinuous Bottom Geometry. *Journal of Computational Physics.* 2008;227(6):3212–3243.

18. Lefloch Philippe G, Thanh Mai Duc. The Riemann problem for the shallow water equations with discontinuous topography. *Communications in Mathematical Sciences.* 2007;5(4):865–885.

19. Pares Carlos, Pimentel Ernesto. The Riemann problem for the shallow water equations with discontinuous topography: The wet–dry case. *Journal of Computational Physics.* 2019;378:344–365.

20. Temple G. Course of theoretical physics, vol. VI, fluid mechanics By L. D. Landau and E. M. Lifshitz (translated by J. B. Sykes and W. H. Reid). Pp. x + 536. Pergamon Press Ltd, London. 1959. E5 5s. net. *Endeavour.* 1960;19(76):228.

21. Toro Eleuterio F.. *Riemann solvers and numerical methods for fluid dynamics : a practical introduction*. Springer,; .

22. Peter D. *Hyperbolic systems of conservation laws and the mathematical theory of shock waves /.* Society for Industrial and Applied Mathematics,; 1973.

23. Liu T G, Khoo Boo Cheong, Wang C W. The ghost fluid method for compressible gas-water simulation. *Journal of Computational Physics.* 2005;204(1):193–221.

24. Godunov Sergei, Bohachevsky I. Finite difference method for numerical computation of discontinuous solutions of the equations of fluid dynamics. *Matematicheskii Sbornik.* 1959;(3):271–306.

25. Greenberg J M, Leroux A Y, Baraille R, Noussair A. Analysis and Approximation of Conservation Laws with Source Terms. *SIAM Journal on Numerical Analysis.* 1997;34(5):1980–2007.

26. Jin Shi, Wen Xin. Two Interface-Type Numerical Methods for Computing Hyperbolic Systems with Geometrical Source Terms Having Concentrations. *SIAM Journal on Scientific Computing.* 2005;26(6):2079–2101.